Hindawi Publishing Corporation
Journal of Nanomaterials
Volume 2015, Article ID 692182, 6 pages
http://dx.doi.org/10.1155/2015/692182

Research Article

Formation and Photocatalytic Activity of $BaTiO_3$ Nanocubes via Hydrothermal Process

Xinrun Xiong, Ruoming Tian, Xi Lin, Dewei Chu, and Sean Li

School of Materials Science and Engineering, University of New South Wales, Sydney, NSW 2052, Australia

Correspondence should be addressed to Ruoming Tian; r.tian@unsw.edu.au and Dewei Chu; d.chu@unsw.edu.au

Received 31 October 2014; Revised 13 January 2015; Accepted 14 January 2015

Academic Editor: Mohammadreza Shokouhimehr

We reported a facile hydrothermal approach to synthesize $BaTiO_3$ nanocubes with controlled sizes for degradation of methylene blue (MB). The nanocubes with reaction time of 48 hours exhibited the highest photocatalytic efficiency, owing to their narrower size distribution and better crystallinity compared to those of 24 hours and, at the meantime, smaller particle size than those of 72 hours. This work also demonstrated the degradation of methylene orange (MO) using $BaTiO_3$ nanocubes synthesized for 48 hours. Compared with the removal of MB, $BaTiO_3$ had lower photocatalytic activity on MO, mainly due to the poorer absorption behavior of MO on the surface of $BaTiO_3$ nanocubes. The degradation efficiency for each photocatalytic reaction was calculated. The possible mechanism of the photocatalytic decomposition on MB has been addressed as well.

1. Introduction

In recent years, the elimination of toxic chemicals from wastewater has become increasingly important. In particular, it has been reported that 17–20% of all industrial water comes from the dyeing and treatment of textiles [1–4]. The problem of toxicity from dye wastewater has received considerable attention, and until now numerous physical or chemical remedies have been developed, such as membrane filtration, ion exchange, and absorption on activated carbon to treat dye wastewaters, whereas they are accompanied with disadvantages of producing concentrated sludge production, low efficiency, and high cost, respectively [1, 5]. Consequently, photocatalysis has been intensively studied owing to its simplicity, low toxicity, good chemical stability, and high degradation efficiency of the dye macromolecule [2, 4, 6].

In particular, oxide photocatalyst has drawn much attention for degrading organic chemicals from wastewater through the advanced oxidation process (AOP), generally with the assistance of UV irradiation. The dye macromolecule can be mineralized into smaller and less harmful substances through a sequence of advanced oxidation processes triggered by strong oxidizing species, such as •OH radicals produced *in situ* [2]. Among these oxides, perovskite-type materials have unique potential which displays photostability and preeminent photocatalytic activity, by virtue of possessing larger lattice distortion and defects, and therefore providing additional routes of trapping holes and inhibiting the recombination rate of electron-hole pairs [4, 6, 7]. Also the vacancy of metal cations and O^{2-} anions in the perovskite-type structure promotes the adsorption of oxygen onto the cation sites of the surface, which boosts the photocatalytic reaction [7, 8].

$BaTiO_3$ is a typical perovskite photocatalyst with unique physical and chemical properties, which highly depend on its morphology and particle size; thus high purity and nanoscale structure are highly desired [9]. Hydrothermal method is being used for the fabrication of perovskite oxide nanocrystals due to several advantages of high purity, homogeneous, crystalline, controllable particle size, and well-defined morphology [10, 11]. Preparation of various $BaTiO_3$ nanostructures such as nanowires, nanocubes, and nanorods has been reported in the literatures [9, 12–15]. Among all these structures, cubic structure has a superior property to decrease crystal defects and enhance the surface-to-volume ratio. Conventionally, $BaTiO_3$ nanocubes have been prepared by several growth methods: sol-gel methods, the conventional hydrothermal method, and recently the surfactant-assisted

hydrothermal method [4, 9, 14–18]. The surfactant assisted hydrothermal method enables growing $BaTiO_3$ nanocubes at lower temperature and the ease of controlling the size and morphology of the final product [13]. By controlling the shape and size of the $BaTiO_3$ nanocrystals, the electronic structure and surface structure are considered to promote the photocatalyst activity. From the electronic structure aspect, smaller nanoparticles have size-dependent electronic states different from the bulk, which guarantee their unique properties [6, 11]. From the surface structure aspect, the cubic shaped nanoparticles have surfaces with well-defined atomic arrangements. The atomic arrangement on the crystal surface can influence the photocatalytic properties in terms of activity and selectivity [1].

Here, in this study, ultrasmall $BaTiO_3$ nanocubes have been successfully fabricated using hydrothermal method. The effect of the reaction time on the size and morphology of the nanocubes was studied. Also, the photocatalytic activity of the as-prepared $BaTiO_3$ nanoparticles on decomposition of methylene blue (MB) and methylene orange (MO) has been investigated.

2. Experimental

All chemicals were used as received without further purification. In a typical synthesis, $Ba(OH)_2$ and TALH (0.05 mol L^{-1}, Ba : Ti = 1 : 1) were dissolved into small amount of distilled water. 6 mL of 1 M NaOH was added to adjust the pH value of the solution to 13. *tert*-butylamine and oleic acid were then added to the solution in sequence (Ba : oleic acid : *tert*-butylamine = 1 : 8 : 12 in molar ratio). Finally, the volume of the solution was adjusted to 30 mL. The resultant mixture was then transferred and sealed into autoclave at 200°C for 24 hrs, 48 hrs, and 72 hrs, respectively. After the hydrothermal process, the final product was washed using ethanol for four times.

As-prepared $BaTiO_3$ products were characterized by X-ray diffraction using CuKa radiation in a 2θ range from 10 to 90 degree with a step size of 0.026. Morphology features of $BaTiO_3$ products were investigated using TEM (Phillips CM200).

The photocatalytic activity of as-prepared $BaTiO_3$ for decomposing methylene blue (MB) and methylene orange (MO) in aqueous solution was investigated by the bleaching of dye solvated. In a typical measurement, the obtained $BaTiO_3$ powders were put into a quartz reactor with 60 mL of MB aqueous solution, and the initial concentration was 20 mg/L. The reactor was then kept in the dark with agitation for 30 min to obtain adsorption equilibrium, prior to light irradiation by a 110 W UV lamp. The efficiency of the degradation processes was evaluated by monitoring the dye decolorization at the maximum absorption around λ = 663 nm as a function of irradiation time in the separated MB solution with a UV-vis spectrometer (Perkin Elmer Lambda 950).

3. Results and Discussion

3.1. Characterization. Figure 1 shows the XRD patterns of samples prepared under different reaction times. It can be found that the samples showed a series of well-indexed peaks referred to as cubic structure. $BaTiO_3$ crystalline phase contents can be observed with all the reaction times. However, a small amount of $BaCO_3$ was also identified in all of the samples contributing to the reaction between $Ba(OH)_2$ and airborne CO_2, which dissolved as CO_3^{2-} during the hydrothermal process [9, 13]. The phase of $BaCO_3$ has been illustrated on the XRD results indexed as the weak peaks at $2\theta = 35^\circ$ and 42°.

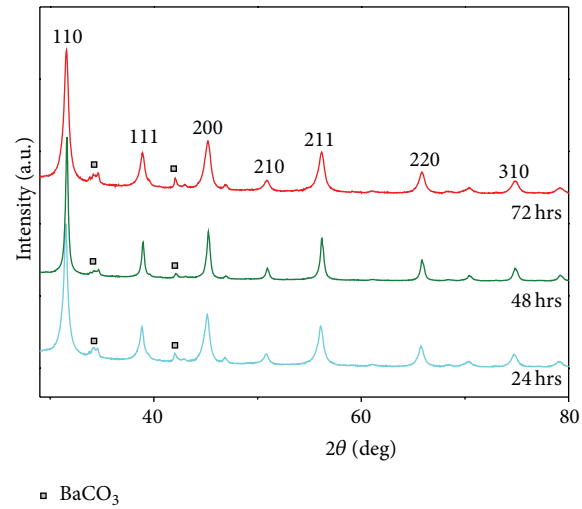

Figure 1: XRD patterns of the $BaTiO_3$ nanoparticles synthesized for different reaction times.

The influence of reaction time on the evaluation of $BaTiO_3$ nanocube was studied by performing the experiments with various reaction times ranging from 24 hrs to 72 hrs, maintaining other reaction parameters identical. According to the TEM images shown in Figure 2, the morphology of all $BaTiO_3$ samples resembles a cube-like nanostructure. The particle size increased from 10 to 20 nm with an increase in synthesis duration, confirming that the particle size of as-prepared $BaTiO_3$ can be tailored by varying the synthesis time. Also, with the increasing reaction time, the edges of the cube became sharper, indicating an increase in the crystallinity of the cubic phase. As shown in Figure 2, little nanocube formation was observed at shorter period of time (24 hrs); instead, particles agglomerated in a spherical shape. Subsequently, by extending the reaction time to 48 hrs, it can be clearly observed that these nanostructures became larger and a few aggregated small particles were found on the surface. By prolonging the reaction time to 72 hrs, well-defined $BaTiO_3$ nanocubes with sharp corners were obtained.

3.2. Degradation of Dyes. The photocatalytic degradation of MB was selected to evaluate the photocatalytic activities of the prepared $BaTiO_3$ nanocubes using UV-vis spectrometer. The band gap of $BaTiO_3$ is E_g = 3.2 eV [19], which allows it to adsorb the UV light. Figure 3 shows typical absorption spectra of methylene blue during different degradation periods. As can be seen from Figure 3, the decreasing absorption value

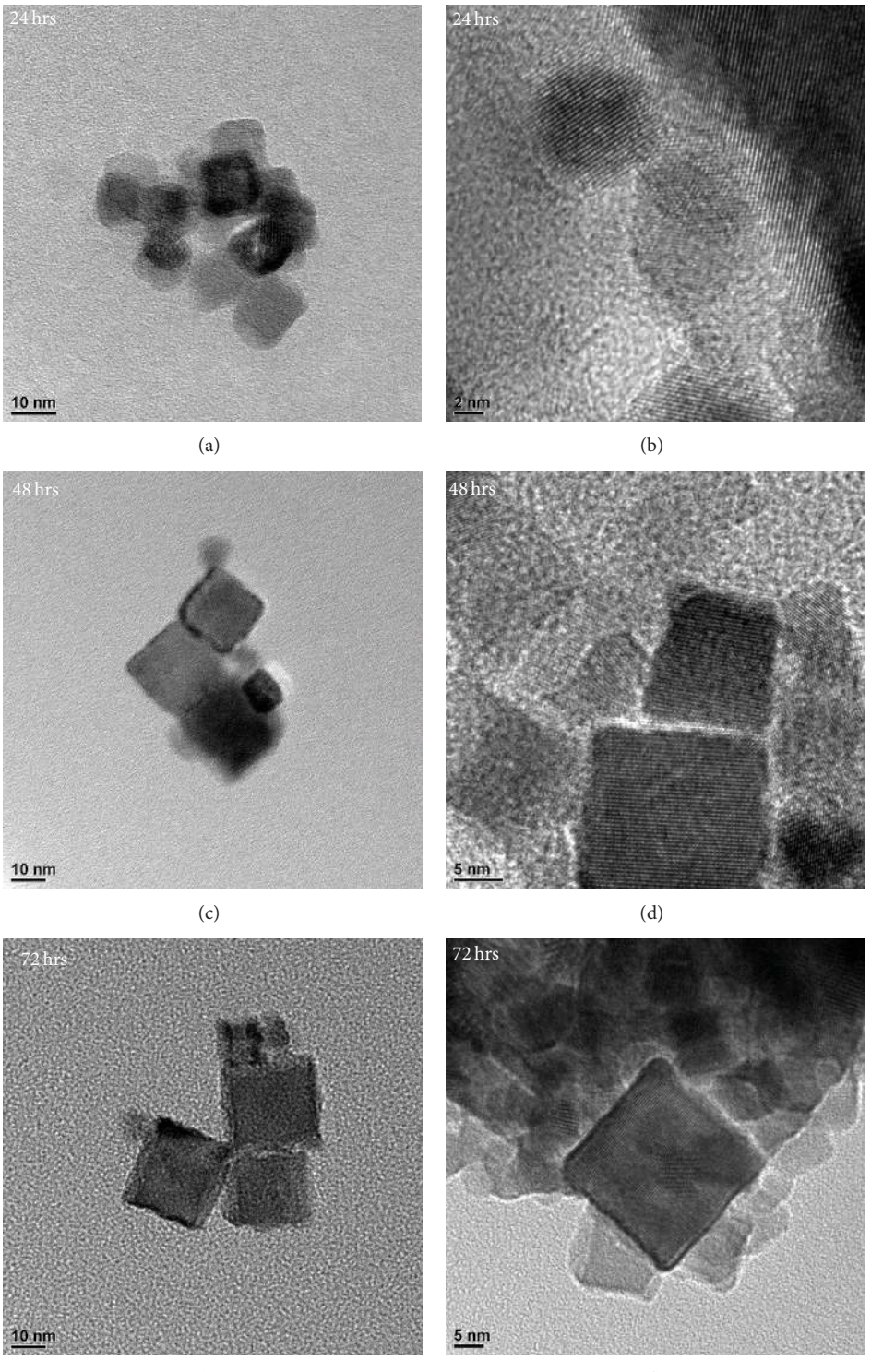

Figure 2: TEM images of the $BaTiO_3$ particles synthesized for 24 hrs, 48 hrs, and 72 hrs.

(A) with the irradiation time represented the reduction of dye concentration in aqueous solution.

The intensity of maximum absorption ($\lambda = 663$ nm) was recorded at different time intervals and converted to the concentration of MB solution. The photocatalytic activities of $BaTiO_3$ synthesized at different reaction durations are exhibited in Figure 4.

As shown in Figure 4, the photocatalytic activities varied from the samples prepared for increasing reaction duration. The sample synthesized for 48 hrs exhibits a relatively higher

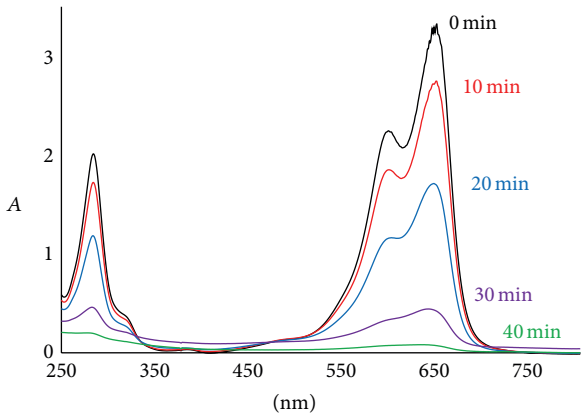

Figure 3: UV-vis absorption spectra of methylene blue using $BaTiO_3$ nanocubes synthesized for 48 hrs as a photocatalyst.

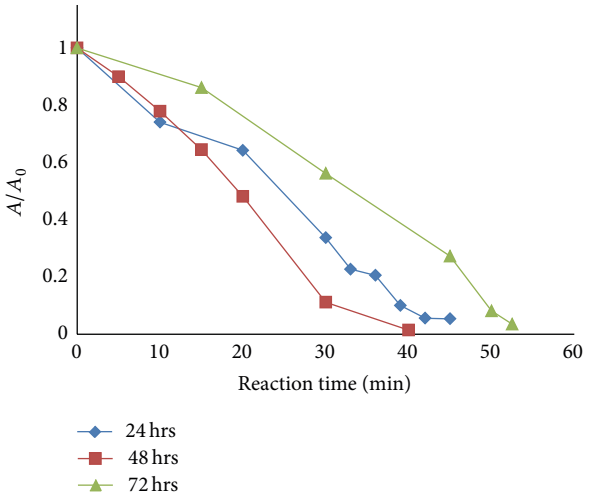

Figure 4: The variation of photocatalytic concentration of methylene blue dye as a function of irradiation time (min) over $BaTiO_3$ samples synthesized for 24 hrs, 48 hrs, and 72 hrs, respectively.

photocatalytic performance than that synthesized for either shorter or longer period. After 40 min of UV illumination, the MB removal over $BaTiO_3$ for 48 hrs is as low as 98%, whereas it takes as long as 55 min until the MB was completely decomposed by $BaTiO_3$ synthesized over a period of 72 hrs.

The photocatalytic activity of $BaTiO_3$ nanocubes for the degradation of methylene orange was conducted under the UV light, shown in Figure 5. Typically, $BaTiO_3$ synthesized for 48 hrs was selected since it provided the optimal photocatalytic performance over the degradation of MB. Compared with the photocatalytic results obtained for degradation of methylene blue, MO was decomposed more slowly by $BaTiO_3$ nanocubes. It took about 65 min of UV illumination to reach a 96% removal.

The degradation efficiency (%) has been calculated and presented in Table 1, defined as

$$\text{Efficiency}\,(\%) = \frac{C_0 - C}{C_0} \times 100, \quad (1)$$

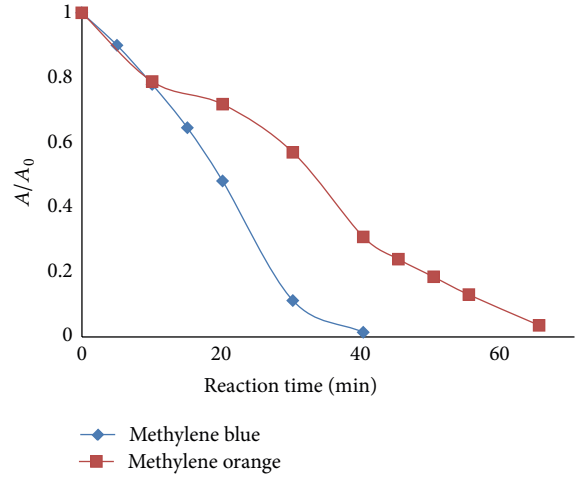

Figure 5: The variation of photocatalytic concentration of MB dye and MO dye as a function of irradiation time (min) over $BaTiO_3$ samples synthesized for 48 hrs and 72 hrs.

Table 1: Degradation efficiency of MB and MO over $BaTiO_3$ nanocubes under 45 min UV irradiation.

Samples	Efficiency (MB)	Efficiency (MO)
$BaTiO_3$ for 24 hrs	94.6%	—
$BaTiO_3$ for 48 hrs	99.2%	76.2%
$BaTiO_3$ for 72 hrs	72.7%	—

where C_0 is the initial concentration of the dye and C is the concentration of dye at degradation time, t.

For the removal of MB, $BaTiO_3$ synthesized for 48 hrs has the highest degradation efficiency which is 99.2% after 45 min UV irradiation. $BaTiO_3$ for 72 hrs has the lowest efficiency of 72.7% under the same period of irradiation time. The intrinsic activity discrepancy among the $BaTiO_3$ nanoparticles prepared over different reaction times can be explained through several factors: particle morphology, particle size, and crystallinity. It is well understood that morphology and size of nanoparticles are the two most important impacts on the photocatalytic activity due to the difference in surface area, the number of the active sites, and consequently the catalytic selectivity [6, 8, 20–22]. In comparison of as-prepared $BaTiO_3$ samples, the nanoparticles prepared for 48 hrs have a better and uniform morphology distribution compared to those synthesized for 24 hrs. Also by synthesizing the $BaTiO_3$ nanocubes for extended reaction duration, higher crystallization can be achieved and therefore, in turn, suppress the recombination of photoinduced holes and electrons [6]. On the other hand, the $BaTiO_3$ nanocubes synthesized for 48 hrs have a smaller size of 15 nm compared to those prepared for 72 hrs. Smaller nanoparticles result in a larger surface area with more active sites and therefore enhance the photocatalytic activity. Also the smaller the particle size, the wider the band gap. Consequently the oxidizing ability of photoexcited holes and the reducing ability of photoexcited electrons are expected to be stronger. Also the migrating time of photoexcited electrons and holes from the inner to

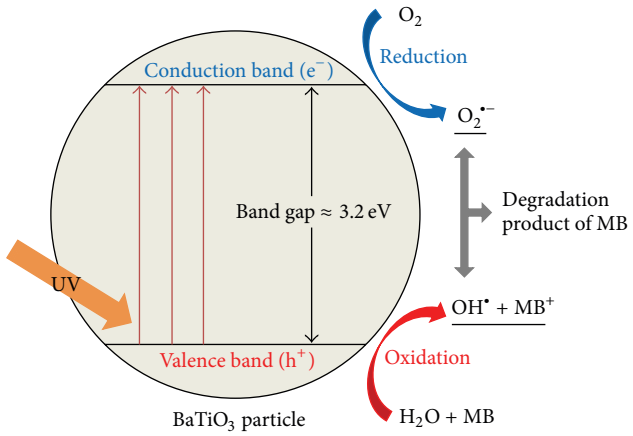

FIGURE 6: Degradation mechanism of MB on $BaTiO_3$ nanocubes.

surfaces is shorter for smaller particle size [20, 21]. Hence the $BaTiO_3$ nanoparticles synthesized for 48 hrs have the highest photocatalyst activity in degradation of MB with smaller crystal size of 15 nm compared to the $BaTiO_3$ synthesized for 72 hrs and with better cubic morphology and crystallinity compared to the $BaTiO_3$ nanoparticles prepared for 24 hrs.

For the removal of MO, the degradation efficiency was as low as 76.2% using $BaTiO_3$ nanocubes synthesized for 48 hrs as a photocatalyst. As the photocatalytic procedure carried out for the removal of MO was identical to that used for MB (the initial dye concentration, the dosage of $BaTiO_3$ powder, and the initial solution pH were identical), the main reason for this degeneracy of the removal efficiency of MO compared to that of MB can be attributed to the chemical structures of MO and MB. It is well known that MB has a positive charged surface whereas MO is negatively charged [23]. The opposite charged surface of these two dyes may lead to a difference in the degree of adsorption on the surface of $BaTiO_3$ nanocubes [23, 24].

3.3. Degradation Mechanism. The mechanism of photocatalysis is shown in Figure 6 and can be described as follows. Under the illumination of UV light irradiation ($h\nu > E_g = 3.2$ eV), the $BaTiO_3$ nanoparticles are photoexcited, promoting charge separation. The electron generated from charge separation will be promoted from the valence band to the conduction band generating. The conduction band electron can migrate to the surface of $BaTiO_3$. Subsequently, oxygen adsorbed on the surface of $BaTiO_3$ is able to react with the photoelectron to initiate a series of strong oxidative free radicals. At the meantime, a positive charged hole (h^+) in the valence band is formed which can react with H_2O to generate •OH radical. These generated radicals further react with MB producing a whole range of intermediates to achieve complete mineralization with the formation of less harmful carbon dioxide, water, and nitrogen [2, 25].

4. Conclusion

Nanocubic $BaTiO_3$ particles were synthesized by hydrothermal methods using *tert*-butylamine and oleic acid as two surfactants. The results of TEM images show that the morphology and size of $BaTiO_3$ nanoparticles can be tailored by changing the reaction time. By increasing the reaction duration, the $BaTiO_3$ particles formed more cubic shape with sharp corners and the particle size increased from 10 nm to 20 nm. These results indicate that $BaTiO_3$ synthesized for 48 hrs has the highest photocatalytic activity, which can be attributed to the relatively better morphology compared to the $BaTiO_3$ synthesized for 24 hrs and smaller particle size compared with the $BaTiO_3$ synthesized for 72 hrs. In addition, the photocatalytic degradation of MO was examined using $BaTiO_3$ photocatalyst. In contrast to cationic MB, anionic MO has lower degradation efficiency on $BaTiO_3$ nanocubes, indicating that the intrinsic charge of dye may lead to a difference in the adsorption behaviour on the surface of photocatalyst.

Conflict of Interests

The authors declare that there is no conflict of interests regarding the publication of this paper.

References

[1] M. R. Hoffmann, S. T. Martin, W. Choi, and D. W. Bahnemann, "Environmental applications of semiconductor photocatalysis," *Chemical Reviews*, vol. 95, no. 1, pp. 69–96, 1995.

[2] S. H. S. Chan, T. Y. Wu, J. C. Juan, and C. Y. Teh, "Recent developments of metal oxide semiconductors as photocatalysts in advanced oxidation processes (AOPs) for treatment of dye waste-water," *Journal of Chemical Technology and Biotechnology*, vol. 86, no. 9, pp. 1130–1158, 2011.

[3] M. A. Rauf and S. S. Ashraf, "Radiation induced degradation of dyes—an overview," *Journal of Hazardous Materials*, vol. 166, no. 1, pp. 6–16, 2009.

[4] W. W. Lee, W.-H. Chung, W.-S. Huang et al., "Photocatalytic activity and mechanism of nano-cubic barium titanate prepared by a hydrothermal method," *Journal of the Taiwan Institute of Chemical Engineers*, vol. 44, no. 4, pp. 660–669, 2013.

[5] T. Robinson, G. McMullan, R. Marchant, and P. Nigam, "Remediation of dyes in textile effluent: a critical review on current treatment technologies with a proposed alternative," *Bioresource Technology*, vol. 77, no. 3, pp. 247–255, 2001.

[6] A. Mills and S. Le Hunte, "An overview of semiconductor photocatalysis," *Journal of Photochemistry and Photobiology A: Chemistry*, vol. 108, no. 1, pp. 1–35, 1997.

[7] M. A. Peña and J. L. G. Fierro, "Chemical structures and performance of perovskite oxides," *Chemical Reviews*, vol. 101, no. 7, pp. 1981–2018, 2001.

[8] T. Seiyama, N. Yamazoe, and K. Eguchi, "Characterization and activity of some mixed metal oxide catalysts," *Industrial & Engineering Chemistry, Product Research and Development*, vol. 24, no. 1, pp. 19–27, 1985.

[9] S. Adireddy, C. Lin, B. Cao, W. Zhou, and G. Caruntu, "Solution-based growth of monodisperse cube-like $BaTiO_3$ colloidal nanocrystals," *Chemistry of Materials*, vol. 22, no. 6, pp. 1946–1948, 2010.

[10] W. Shi, S. Song, and H. Zhang, "Hydrothermal synthetic strategies of inorganic semiconducting nanostructures," *Chemical Society Reviews*, vol. 42, no. 13, pp. 5714–5743, 2013.

[11] T.-D. Nguyen, "From formation mechanisms to synthetic methods toward shape-controlled oxide nanoparticles," *Nanoscale*, vol. 5, no. 20, pp. 9455–9482, 2013.

[12] N. Bao, L. Shen, G. Srinivasan, K. Yanagisawa, and A. Gupta, "Shape-controlled monocrystalline ferroelectric barium titanate nanostructures: from nanotubes and nanowires to ordered nanostructures," *Journal of Physical Chemistry C*, vol. 112, no. 23, pp. 8634–8642, 2008.

[13] F. Dang, K. Mimura, K. Kato et al., "*In situ* growth $BaTiO_3$ nanocubes and their superlattice from an aqueous process," *Nanoscale*, vol. 4, no. 4, pp. 1344–1349, 2012.

[14] W. Sun, J. Li, W. Liu, and C. Li, "Preparation of fine tetragonal barium titanate powder by a microwave-hydrothermal process," *Journal of the American Ceramic Society*, vol. 89, no. 1, pp. 118–123, 2006.

[15] H. Xu, L. Gao, and J. Guo, "Hydrothermal synthesis of tetragonal barium titanate from barium chloride and titanium tetrachloride under moderate conditions," *Journal of the American Ceramic Society*, vol. 85, no. 3, pp. 727–729, 2002.

[16] C. Pithan, D. Hennings, and R. Waser, "Progress in the synthesis of nanocrystalline $BaTiO_3$ powders for MLCC," *International Journal of Applied Ceramic Technology*, vol. 2, no. 1, pp. 1–14, 2005.

[17] A. S. Bhalla, R. Guo, and R. Roy, "The perovskite structure—a review of its role in ceramic science and technology," *Materials Research Innovations*, vol. 4, no. 1, pp. 3–26, 2000.

[18] C. Y. Su, Y. Otsuka, C. Y. Huang et al., "Grain growth and crystallinity of ultrafine barium titanate particles prepared by various routes," *Ceramics International*, vol. 39, no. 6, pp. 6673–6680, 2013.

[19] M. Cardona, "Optical properties and band structure of $SrTiO_3$ and $BaTiO_3$," *Physical Review*, vol. 140, no. 2A, pp. A651–A655, 1965.

[20] S. Li, L. Jing, W. Fu, L. Yang, B. Xin, and H. Fu, "Photoinduced charge property of nanosized perovskite-type $LaFeO_3$ and its relationships with photocatalytic activity under visible irradiation," *Materials Research Bulletin*, vol. 42, no. 2, pp. 203–212, 2007.

[21] L. Jing, Z. Xu, X. Sun, J. Shang, and W. Cai, "The surface properties and photocatalytic activities of ZnO ultrafine particles," *Applied Surface Science*, vol. 180, no. 3-4, pp. 308–314, 2001.

[22] A. V. Emeline, V. N. Kuznetsov, V. K. Ryabchuk, and N. Serpone, *Heterogeneous Photocatalysis: Basic Approaches and Terminology*, Elsevier, 2013.

[23] R. Gong, J. Ye, W. Dai et al., "Adsorptive removal of methyl orange and methylene blue from aqueous solution with finger-citron-residue-based activated carbon," *Industrial and Engineering Chemistry Research*, vol. 52, no. 39, pp. 14297–14303, 2013.

[24] A. Ajmal, I. Majeed, R. N. Malik, H. Idriss, and M. A. Nadeem, "Principles and mechanisms of photocatalytic dye degradation on TiO_2 based photocatalysts: a comparative overview ," *RSC Advances*, vol. 4, no. 70, pp. 37003–37026, 2014.

[25] A. Houas, H. Lachheb, M. Ksibi, E. Elaloui, C. Guillard, and J.-M. Herrmann, "Photocatalytic degradation pathway of methylene blue in water," *Applied Catalysis B: Environmental*, vol. 31, no. 2, pp. 145–157, 2001.